Detection and Discrimination of Inter-Turn and Demagnetization faults for PMSMs Based on An FEM and Model-Based Technique

Yacine Maanani
Département de génie électrique
École de technologie supérieure
Montréal, Canada
yacine.maanani@gmail.com

Qingsong Wang
Département de génie électrique
École de technologie supérieure
Montréal, Canada
qingsong.wang@etsmtl.ca

***Abstract*—This study introduces a combined diagnostic approach that merges analytical modeling with finite element analysis (FEA) to identify and differentiate between inter-turn short-circuit and demagnetization faults in permanent magnet synchronous motors (PMSMs). It analyzes the magnetic field behavior near the stator windings using both a dynamic mathematical model and a two-dimensional FEA simulation. The analytical model outlines how the motor responds under both normal and faulty conditions, while the FEM model built in ANSYS provides a visual representation of how the magnetic field changes based on the type and severity of the fault. By examining the magnetic flux density and field intensity in matching areas of the stator, the method develops a diagnostic index that quantifies the extent of the fault. The findings show that this hybrid approach can accurately detect and distinguish between different PMSM faults with a high degree of reliability.**

Keywords—Permanent Magnets Synchronous Machine (PMSM), Finite Element Method (FEM), Interturn short-circuit (ITSC), Demagnetization, structural analysis, Fast Fourier Transform (FFT).

I. INTRODUCTION

The high power density, high efficiency, and ease of control that are inherent in permanent magnet synchronous machines (PMSMs) have led to their widespread use in industry. There are serious dependability issues with the quick and extensive deployment of PMSMs, especially for mission and safety-critical systems.

Once a defect has been started, it can lead to expensive operating losses, severe performance decline, or even deadly accidents. To identify post-failure safe operating zones, create trustworthy diagnosis algorithms, and mitigation strategies, it is crucial to get the fault characterisation of PMSMs. One of the most common and difficult-to-notice PMSM failures that can result in serious issues is the interturn short circuit fault [1]. The permanent magnets' irreversible demagnetization is the machine's most sensitive cost concern when the temperature is too high [2]. Both the temperature of the magnets and the magnetic field produced by the winding currents combine to cause the irreversible demagnetization. Early aging and irreversible demagnetization result from a decrease in winding current as the magnets' temperature rises. As a result, one of the PMSM's main advantages its torque density decreases.

Demagnetization in PMSMs can be mitigated by controlling current and temperature or by increasing design safety margins. Since higher margins raise drive cost, this study investigates PMSM performance and magnetic stability under demanding operating conditions to improve reliability without excessive design constraints. Because of the high circulating current that flows in the shorted circuit, the most common electrical defect in PMSMs is the inter-turn short circuit (ITSC) fault, which is also very important. The problem is brought on by vibrations, heat stress, and voltage stress, and the ITSC happens when the insulation between neighboring stator winding coils deteriorates [3]. In most cases, deteriorating insulation is simulated using a fault resistance R_f and a fault turn ratio μ. The short circuit drives the high circulating current, produces excessive heat, this results in a localized reversal of the magnetic field, all of which might exacerbate the fault. It is necessary to increase the current to maintain a certain load torque when ISF happens. Plant failure or monetary losses might result from an increase in the circulating current [4]. Therefore, early identification and monitoring of demagnetization is crucial to avoiding expensive maintenance expenses and downtime.

To find demagnetization and ITSC defects in PMSMs, many methods have been used [4] have used a signal-based approach to track vibration in order to study the behavior of ITSC and demagnetization faults. Additionally, Real-time application of FEM-based models is difficult and computationally demanding. Thus, structural analysis is suggested as a substitute method for identifying and separating different types of defects in a complex system without the need for an in-depth understanding of the dynamics of the system [5].

This study focuses on two common faults in PMSMs demagnetization and inter-turn short-circuit (ITSC) with the aim of accurately detecting and distinguishing between them. A dynamic PMSM model formulated in the ABC reference frame is employed, in which additional terms are incorporated to represent the effects of ITSC and demagnetization faults within the governing equations. The modified three-phase flux and voltage equations account for these added effects, reflecting the changes in the permanent-magnet flux linkage caused by demagnetization and the alterations in stator resistance and inductance resulting from an inter-turn short-circuit fault. Additionally, An algorithm based on the finite element method (FEM) was developed as a fault diagnosis technique to measure the magnetic field surrounding the winding geometry structural analysis of PMSMs in order to detect and evaluate the severity of inter-turn short circuits in the winding and demagnetization.

II. PMSM MODEL IN HEALTHY AND FAULTY STATES

A faulty situation with a healthy state and an interturn short-circuit fault is derived using the PMSM model in this section.

A. PMSM model under ITSC in the abc frame.

979-8-3315-8138-1

Under healthy operating conditions, the three-phase terminal voltages of the PMSM in the stationary reference frame can be formulated as follows:

$$V_s = [R_s].[I_s] + [L_{ss}]\frac{d}{\mathrm{dt}}[I_s] + [E_s] \tag{1}$$

The symbols depict the back-EMF, stator voltage, and current vectors $[V_s]$, $[I_s]$, and $[E_s]$:

$$V_s = [v_a\ \mathrm{v}_b\ \mathrm{v}_c]^T,\ I_s = [I_a\ \mathrm{I}_b\ \mathrm{I}_c]^T,\ E_s = [e_a\ \mathrm{e}_b\ \mathrm{e}_c]^T \tag{2}$$

They denote the back-EMFs, stator currents, and three-phase voltages, respectively. The parameters R and L correspond to the stator phase resistance and inductance. In the *abc* frame, the motor model in defective state may be expressed as (3), incorporating the defective parts that were created during the motor stages [6].

$$\begin{bmatrix} V_a \\ V_b \\ V_c \\ 0 \end{bmatrix} = \begin{bmatrix} R & 0 & 0 & -R_{af} \\ 0 & R & 0 & 0 \\ 0 & 0 & R & 0 \\ -R_{af} & 0 & 0 & -R_{af}+r_f \end{bmatrix}\begin{bmatrix} i_a \\ i_b \\ i_c \\ i_f \end{bmatrix} + \begin{bmatrix} e_a \\ e_b \\ e_c \\ -e_f \end{bmatrix} \tag{3}$$

$$+\begin{bmatrix} L & M & M & -(L_{af}+M_{ahaf}) \\ 0 & R & 0 & -M_{afb} \\ 0 & 0 & R & -M_{afc} \\ -(L_{af}+M_{ahaf}) & -M_{afb} & -M_{afc} & L_{af} \end{bmatrix}$$

$$\begin{cases} e_f = \mu e_f, \\ R_{af} = (1-\mu)R \\ L_{af} = (1-\mu)^2 L \\ M_{ahaf} = \mu(1-\mu)M \end{cases} \tag{4}$$

Where V_a, V_b,V_c, i_a, i_b, i_c and e_a, e_b, e_c includes the addition of the defective parts that were created throughout motor stages ; Self-inductance, mutual-inductance, and stator phase resistance of the healthy machine are shown by R, L, and M, respectively; the resistance and self-inductance of the defective winding a_{sf} are denoted by R_{af} and L_{af}. a_{sh} and the windings a_{sf}, b_s, and c_s, respectively, have mutual inductances called M_{ahaf}, M_{afb}, and M_{afc}; I_f, r_f, and e_f represent fault back EMF, fault resistance, and fault current, respectively.

Furthermore, the PMSM's electromagnetic torque with stator interturn faults can be computed using:

$$T_e = \frac{e_\alpha I_\alpha + e_b I_{sb} + e_c I_{sc} - e_f I_f}{\Omega} \tag{5}$$

where Ω is the mechanical speed.

A. PMSM with stator interturn faults in the αβ Frame

Figure. 1 shows the inter-turn defect of the PMSM machine's stator winding (R_f), whose value fluctuates based on the severity of the problem, is the resistance that replicates the breakdown of the insulation, and (I_f) is the current in the short circuit. Upon approaching zero R_f, the defect becomes a full interturn short circuit.

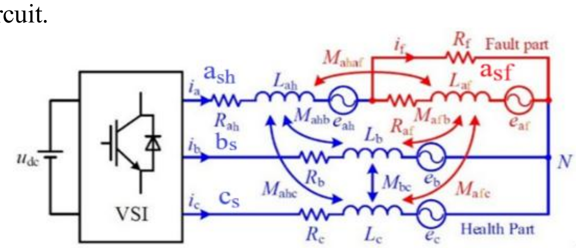

Fig. 1. The equivalent circuit architecture of a three-phase PMSM with a picture of a stator following an ITSC failure in phase a [1].

The stator reference frame changes when the zero sequence component of the stator current from the windings star connection is zero [7]:

$$\begin{bmatrix} x_\alpha \\ x_\beta \end{bmatrix} = \frac{2}{3}\begin{bmatrix} 1 & -\frac{1}{2} & -\frac{1}{2} \\ 0 & \frac{\sqrt{3}}{2} & -\frac{\sqrt{3}}{2} \end{bmatrix}\begin{bmatrix} x_a \\ x_b \\ x_c \end{bmatrix} \tag{6}$$

The simplified inter-turn winding fault equations for the PMSM machine in α, β coordinates are as follows:

$$[V_{\alpha\beta}] = R_s[I_{\alpha\beta}] + [L_{\alpha\beta}]\frac{d}{\mathrm{dt}}[I_{\alpha\beta}] + [e_{\alpha\beta}] - [L'_0]\frac{d}{\mathrm{dt}}[I_f] - [R'_0]I_f \tag{7}$$

For the defective loop (a_{sf}), When α and β are used, the voltage equation becomes true:

$$0 = -\sqrt{\frac{2}{3}}R_{af}I_{as} - \sqrt{\frac{2}{3}}\left(L_{\mathrm{af}} + M_{\mathrm{ahaf}} - \frac{M_{\mathrm{afb}}+M_{\mathrm{afc}}}{2}\right)\frac{\mathrm{d}I_{as}}{\mathrm{dt}} - e_{af}$$

$$-\frac{1}{\sqrt{2}}(M_{\mathrm{afb}} - M_{\mathrm{afc}})\frac{\mathrm{dI}_{bs}}{\mathrm{dt}} - M_{afc}\frac{\mathrm{dI}_{cs}}{\mathrm{dt}} + (R_{af}+r_f)I_f + L_{af}\frac{\mathrm{dI}_f}{\mathrm{dt}} \tag{8}$$

M_{afb} is equivalent to M_{afc} for the machine, where each pole and phase has a single slot. The Clark transform may be used to rewrite (1) as follows:

$$\begin{bmatrix} V_\alpha \\ V_\beta \\ 0 \end{bmatrix} = \begin{bmatrix} R & 0 & -R_{\alpha f'} \\ 0 & R & 0 \\ -R_{\alpha f'} & 0 & R_{\alpha f'}+r_f \end{bmatrix}\begin{bmatrix} I_\alpha \\ I_\beta \\ I_f \end{bmatrix} + \begin{bmatrix} e_\alpha \\ I_\beta \\ -e_f \end{bmatrix} + \begin{bmatrix} L' & 0 & -L_{f'} \\ 0 & L' & 0 \\ -L_{f'} & 0 & L_{af} \end{bmatrix}\frac{d}{dt}\begin{bmatrix} I_\alpha \\ I_\beta \\ I_f \end{bmatrix} \tag{9}$$

$$\begin{cases} R_{\alpha f'} = \frac{2}{3}R_{\alpha f'} \\ L' = L - M \\ L_{f'} = \frac{2}{3}(L_{af} + M_{ahaf} - M_{afb}) \end{cases} \tag{10}$$

Because the sequence component of the current is null, the electromagnetic torque can be expressed as follows:

$$T_e = \frac{e_\alpha I_\alpha + e_\beta I_\beta - e_{\alpha f} I_f}{\Omega} \tag{11}$$

B. PMSM with Demagnetization faults in the abc Reference Frame

The air-gap magnetic field results from the combined effect of the permanent magnet flux and the stator winding current. Hence, any demagnetization in the magnets alters both the shape and amplitude of this field [8].

In the ideal case without harmonics, the non-sinusoidal flux linkage $\lambda_s$exhibits half-wave symmetry and can be expressed as follows:

$$\lambda_s = \begin{bmatrix} \sum_{k=1}^{\infty}\lambda_{2k-1}\cos[(2k-1)\theta_e] \\ \sum_{k=1}^{\infty}\lambda_{2k-1}\cos\left[(2k-1)\left(\theta_e - \frac{2\pi}{3}\right)\right] \\ \sum_{k=1}^{\infty}\lambda_{2k-1}\cos\left[(2k-1)\left(\theta_e + \frac{2\pi}{3}\right)\right] \end{bmatrix} \tag{12}$$

Where λ_{2k-1} symbolizes the harmonic component of flux's amplitude and θ_e represents the electrical angle.

979-8-3315-8138-1

The electromagnetic induction law states that the back EMFs may be computed by

$$e = \frac{d\lambda_s}{dt} = -\frac{d\lambda_s}{d\theta_e}\frac{d\theta_e}{dt} \tag{13}$$

To rewrite the back EMFs, equation (12) should be altered to equation (13) as:

$$e = w_e \begin{bmatrix} \sum_{k=1}^{\infty} \lambda_{2k-1}\, sin[(2k-1)\theta_e] \\ \sum_{k=1}^{\infty} \lambda_{2k-1}\, sin\left[(2k-1)\left(\theta_e - \frac{2\pi}{3}\right)\right] \\ \sum_{k=1}^{\infty} \lambda_{2k-1}\, sin\left[(2k-1)\left(\theta_e + \frac{2\pi}{3}\right)\right] \end{bmatrix} \tag{14}$$

where w_e represents the electrical rotor's angular velocity [8].

Then, Equation (14) can be rewritten as:

$$e = w_e B(\theta_e)\, \lambda_{amp}$$

As indicated by (14), degradation in the magnetic properties of the permanent magnets leads to distortion in both the waveform and magnitude of the back-EMF. The torque expression is derived from the magnetic co-energy while neglecting cogging torque [9].

$$T_e = \frac{d\lambda_s^T}{d\theta_e} i_s = \frac{e^T i_s}{w_m} \tag{15}$$

Let p denote the number of pole pairs, ω_m the mechanical angular velocity, and $\omega_e = p\omega_m$ the electrical angular velocity. Defining $\mu = pB(\theta_e)\lambda_{\text{amp}}$ to represent the back-EMF at unit speed and substituting this into (15), the mechanical equation of the PMSM is obtained to analyze the influence of demagnetization on rotor speed:

$$T_e = j\frac{dw_m}{dt} i_s + T_L + Bw_m \tag{16}$$

III. SIMULATION RESULTS

A. Simulation results in MATLAB/Simulink

Table I presents the principal parameters utilized in the MATLAB/Simulink simulation model, developed by integrating equations (3) and (5) to represent the PMSM operating under an inter-turn short-circuit fault condition.

Table I. MAIN PARAMETERS OF PMSM

Rated Power	P_n	5 kW
Number of pole pairs	p	4
Winding turn no./slot	N*s*	40
Stator resistance	R_s	0.88 Ω
Stator inductance	L_s	2.82mH
Synchronous speed	Ω_s	1000rpm
Inertia moment	J	0.0006 kg.m^2
Coefficient of damping	f	0.007 Nm/rad/s
Flux established by rotor	λ_s	0.108 Wb

Figure 2 presents the simulated performance of the PMSM operating at a rated speed of 1000 rpm under a constant load torque of 10 N·m. An inter-turn short-circuit fault is applied to phase a at t = 2 s, defined by the parameters μ = 0.15 and R_f = 0.01 Ω. The fault creates magnetic and electrical unbalance in the stator windings, leading to an increase in short-circuit current beyond twice its nominal level and causing noticeable distortion in the three-phase currents and back-EMF waveforms. As illustrated in Fig. 3, the inter-turn fault generates a distinct third-harmonic component in the stator current, while the corresponding dq-axis currents reveal pronounced second- and fourth-order harmonic components. These harmonic distortions serve as reliable indicators of ITSC faults. However, because of the machine's high inertia, the electromagnetic torque and rotor speed remain almost unchanged at low-speed operation, despite the presence of significant current harmonics.

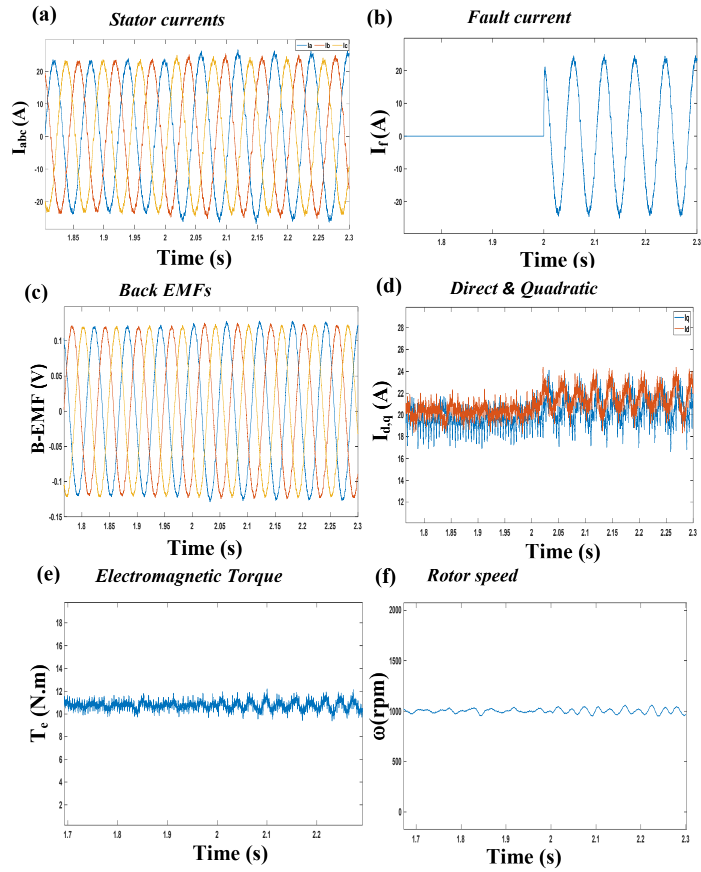

Fig. 2. Variation of the main operating waveforms of the PMSM before and after a 15% inter-turn short-circuit (ITSC) fault.

The rotor in the healthy motor establishes a flux of λs = 0.108 Wb for the demagnetization fault in the PMSM, according to equations (3) and (5) of the fault model. Table. I displays the primary parameters, whereas Fig. 4 displays the simulation results.

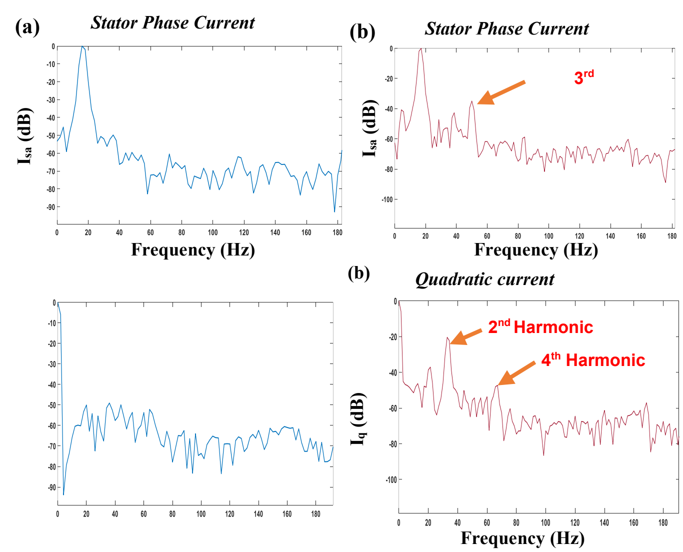

Fig. 3. FFT analysis of the Stator current and the *q*-axis current a) Healthy State b) Faulty State: μ= 50 %, r_f = 0.01 Ω.

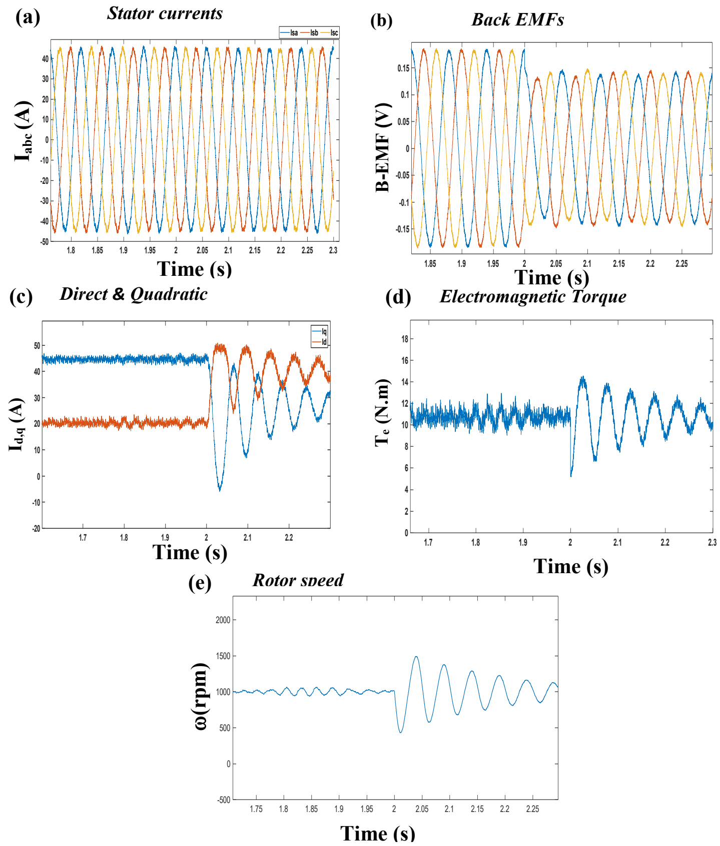

Fig. 4. Variation of the main operating waveforms of the PMSM before and after a 50% demagnetization.

Figure. 4 presents the simulation results of the PMSM operating under a load torque of 10 N·m at a reference speed of 1000 rpm. At t = 2 s, a 50% demagnetization level is applied to the permanent magnets.

Figure. 4 shows how uniform demagnetization affects PMSM performance. While the stator's symmetry ensures balanced three-phase currents, the back-EMF amplitude drops. This leads to distortions in the dq-axis currents, torque, and speed, along with a decrease in their magnitudes. Figure. 5 further reveals that demagnetization introduces a third-harmonic component in the back-EMFs and a second harmonic in the q-axis current. These harmonic signatures demonstrate that analyzing current sequences and spectra can effectively detect demagnetization issues in PMSMs.

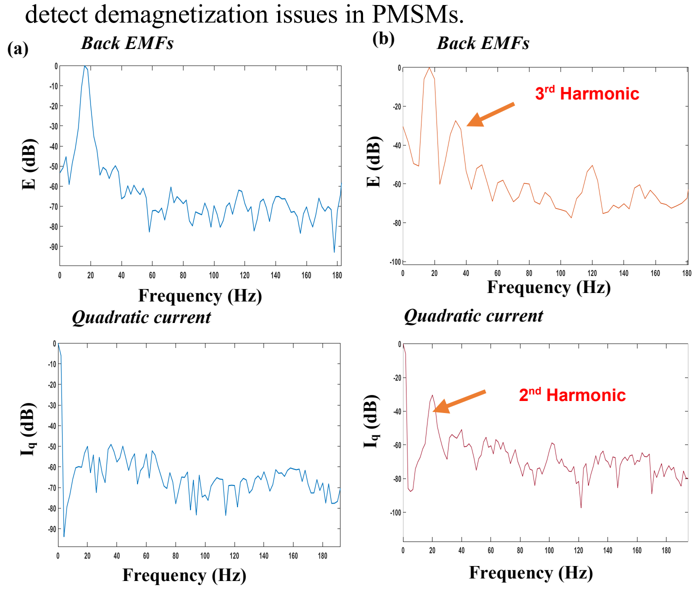

Fig. 5. FFT analysis of the Back EMF and the q-axis current a) Healthy State b) Faulty State: 50 % demagnetization .

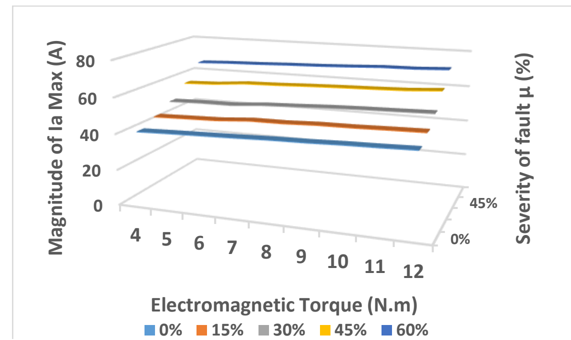

Fig. 6. Stator current analysis for different fault severity levels at 1000 rpm

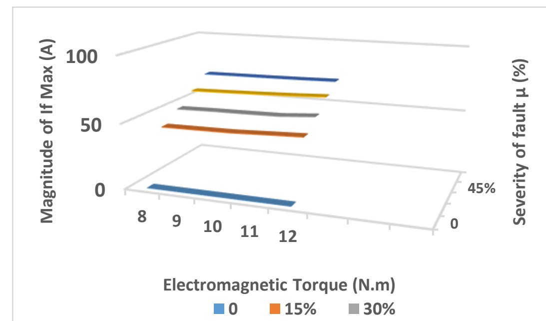

Fig. 7. Fault current analysis for different fault severity levels at 1000 rpm.

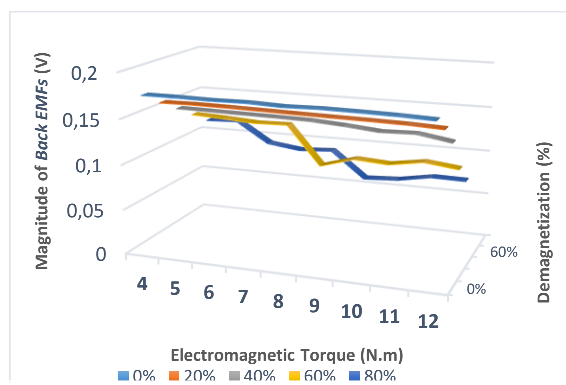

Fig. 8. Magnitude of Back EMFs analysis for different Demagnetization levels at 1000 rpm

To investigate the influence of (ITSC) and demagnetization faults in PMSMs, several tests were conducted under different values of electromagnetic torque (N·m). For the ITSC analysis, the stator current of phase *a* (I_{sa}) and the fault current (I_f) were selected as representative state variables, as illustrated in Figures. 6–7. In addition, different levels of demagnetization faults were considered in order to examine their effect on the magnitude of the back electromotive forces (EMFs) (V) of the PMSM, as presented in Fig. 8. All results were obtained at a constant operating speed of 1000 rpm.

Figure. 6 illustrates the stator current (I_{sa}) of phase *a* . In the healthy state, the magnitude of Isa shows a slight increase; however, as the fault severity grows, the current magnitude rises significantly. Regarding the Electromagnetic Torque (N·m), it can be observed that the ITSC fault has a stronger impact on the current magnitude compared to the healthy condition.

Figure. 7 presents the fault current (I_f). In the healthy state, If remains equal to zero. As the Electromagnetic Torque (N·m) increases, the magnitude of If also increases, highlighting the clear influence of ITSC fault progression.

Figure. 8 shows the variation of Back EMFs under different levels of demagnetization faults. In the healthy condition, the

Back EMFs remain stable with only minor fluctuations as the Electromagnetic Torque (N·m) increases. For 20% and 40% demagnetization faults, a slight decrease in the Back EMFs can be observed with the evolution of torque. However, when the demagnetization level reaches 60%, the Back EMFs decrease by nearly half, clearly revealing the significant impact of severe demagnetization on machine performance.

B. *Simulation results in ANSYS Maxwell*

As illustrated in Fig. 9, the surface-mounted PMSM model under study featuring 48 stator slots and 4 pole pairs was developed in ANSYS Maxwell using the finite element analysis (FEA) method. The key design parameters of the machine are summarized in Table II.

Phase a in the FEM is divided into two sections, the health portion (a_1) and the fault part (a_2), as seen in Fig. 09(b). The short-circuited coil (a_2) is modeled with 80 turns and a resistance of 0.031 Ω, corresponding to a coupling factor of $\mu = 0.25$. Subsequently, this winding is connected to a 2 Ω external resistor to emulate the inter-turn short circuit within the ANSYS Maxwell circuit.

TABLE. II. Main Geometrical Parameters of the PMSM

Parameter	Description	Value
Stator outer diameter	D_{so}	269.24 mm
Stator inner diameter	D_{si}	161.9 mm
Rotor outer diameter	D_{ro}	77.15 mm
Rotor inner diameter	D_{ri}	15 mm
Air-gap length	g	1.93 mm
Stator core length	L_s	162.8 mm
Rotor core length	L_r	131.5 mm
Permanent magnet thickness	t_{PM}	3 mm
Number of coils per phase	N_{ph}	320
Number of slots	N_s	48
Pole pairs	p	4

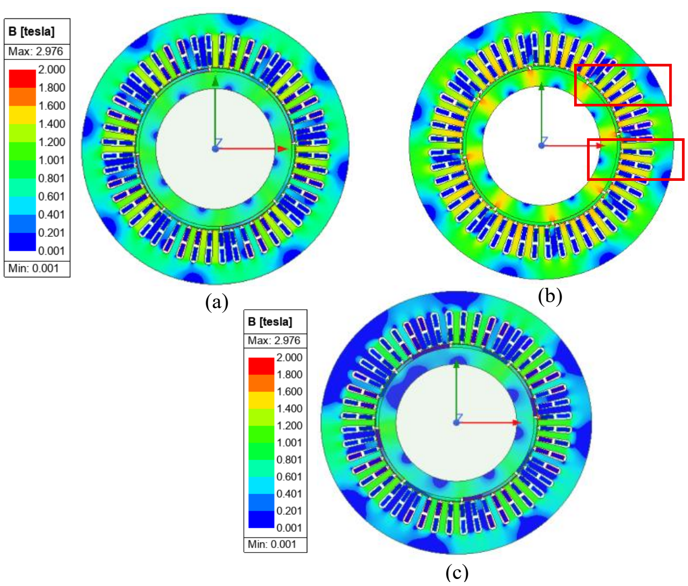

Fig. 9. Magnetic flux density distribution of the PMSM under different operating conditions: (a) healthy model, (b) inter-turn short-circuit (ITSC) fault model, and (c) demagnetization fault model.

In the subject of motor ontology analysis, the FEM is frequently used because it provides a clear visual representation of the magnetic field intensity distribution. Following a quarter of the ITSC, the winding that has been short-circuited generates a circulating current. As the short-circuit current increases, the magnetic flux density in certain stator teeth enters deeper saturation, leading to localized losses within the motor. Figure 9(b) illustrates the magnetic flux density distribution of the machine before and after the occurrence of the fault.

The magnetic flux density pattern of the local demagnetization faults at a 60% demagnetization fault effect for one PMSM pole is shown in Fig. 09c. This image shows that while the magnetic flux density at other locations has hardly changed, demagnetization failure will result in variable degrees of decreases in the PM magnetic field and the space air-gap magnetic density at the relevant place. A demagnetization defect decreases the magnetic field solely around the impacted pole, but an ITSC results in local magnetic saturation and higher losses, according to the FEM study.

IV. Conclusions

This study introduced a FEM-based diagnostic method for identifying and differentiating between demagnetization and inter-turn short-circuit problems in PMSMs. The suggested approach analyzes magnetic field fluctuations under various fault severities by efficiently combining finite element simulations and analytical modeling. Simulation outcomes in ANSYS and MATLAB/Simulink Maxwell showed that circulating currents, magnetic flux distortion, and other phenomena are the main causes of an inter-turn short-circuit failure, higher losses and current imbalance as a result of localized saturation in the stator teeth. Conversely, demagnetization defects result in a notable decrease in the amplitude of the back-EMF and the intensity of the magnetic field surrounding the impacted pole, while adjacent areas are mostly unaffected. The ability to reliably distinguish between the two problem types is made possible by these unique electromagnetic signatures, demonstrating the efficacy of the FEM-based diagnostic system for early fault detection and PMSM status monitoring.

References

[1] Y. Rao, Y. Wang, and W. Wang, "A Simplified Modeling and Analysis Method for Interturn Short-Circuit Fault of Permanent Magnet Synchronous Motor," in *2023 26th International Conference on Electrical Machines and Systems (ICEMS)*, Zhuhai, China: IEEE, Nov. 2023, pp. 4450–4455. doi: 10.1109/ICEMS59686.2023.10345238.

[2] S. H. Ebrahimi, "Real-Time Fault Diagnosis of Permanent Magnet Synchronous Motor and Drive System".

[3] L. Cao and Z. Wu, "On-Line Detection of Demagnetization for Permanent Magnet Synchronous Motor via Flux Observer," *Machines*, vol. 10, no. 5, p. 354, May 2022, doi: 10.3390/machines10050354.

[4] T. J. Dos Santos Moraes, E. Semail, and N.-K. Nguyen, "Demagnetization analysis of an open-end windings 5-phase PMSM under transistor short-circuit fault," in *IECON 2019 - 45th Annual Conference of the IEEE Industrial Electronics Society*, Lisbon, Portugal: IEEE, Oct. 2019, pp. 6206–6211. doi: 10.1109/IECON.2019.8927205.

[5] Y. Zuo, A. Darabi, C. Lai, and K. Lakshmi Varaha Iyer, "Online Interturn Short Circuits Fault Monitoring for Permanent Magnet Synchronous Machines," in *IECON 2022 – 48th Annual Conference of the IEEE Industrial Electronics Society*, Brussels, Belgium: IEEE, Oct. 2022, pp. 1–6. doi: 10.1109/IECON49645.2022.9968716.

[6] L. Cao and Z. Wu, "On-Line Detection of Demagnetization for Permanent Magnet Synchronous Motor via Flux Observer," *Machines*, vol. 10, no. 5, p. 354, May 2022, doi: 10.3390/machines10050354.

[7] [1] Y. Maanan, "PMSM Inter-Turn Short Circuit Fault Diagnosis using EKF Observer and FFT for Sensorless Input-Output Linearization Control," in 2023 International Conference on Electrical Engineering and Advanced Technology (ICEEAT), Batna, Algeria: IEEE, Nov. 2023, pp. 1–7. doi: 10.1109/ICEEAT60471.2023.10426148.

[8] F. Huang *et al.*, "Demagnetization Fault Diagnosis of Permanent Magnet Synchronous Motors Using Magnetic Leakage Signals," *IEEE Trans. Ind. Inf.*, vol. 19, no. 4, pp. 6105–6116, Apr. 2023, doi: 10.1109/TII.2022.3165283.